Optimisation of ray-tracing algorithms for EMF safety assessment of base station installations

Francois du Plessis, Max Birch, Marnus Van Wyk & Frans Meyer

EMSS Consulting (Pty) Ltd,
3 Meson, Stellenbosch, WC, South Africa, 7600
Email: contact@emssixus.com

Abstract - *EMF simulation algorithms using the ray-tracing method (CENELEC EN 50383, IEC 62232) are optimised to radically reduce computation time. Exclusion zone isosurface extraction for the prevention of over-exposure near mobile base-stations is performed using a fast adaptive technique based on the marching tetrahedra method. The algorithms are parallelised and the ray-tracing method is optimized to allow use of a single point source for fast calculation in the approximate far-field.*

Introduction and Objectives

The EU Directive on physical agents, 2004/40/EC [1], makes it mandatory for employers to ensure that employees are not exposed to radiation levels exceeding reference level guidelines such as ICNIRP [2]. Implementing this can be accomplished by means of a combination of simulations and measurements. Inherent uncertainties in measurements are making the speed and accuracy of simulations more attractive, such as those performed in IXUS [3]. Conventional electromagnetic solvers become inefficient with large electrical problems such as multiple transmitting antennas on a base station. However, using the synthetic ray-tracing technique according to CENELEC EN 50383 [4] and IEC 62232 [5], panel and omnidirectional antennas are easily modelled as linear arrays of point sources. This makes it practical to simulate electrically large problems on standard workstations.

Simulation results are displayed in the form of isosurface exclusion zones, indicating where the field values exceed the specified reference levels. It can also be displayed as orthogonal slices (2D plane), or as field values at specified coordinate points. The optimisation of our calculation methods can be broken down into two categories: The efficient selection of the required field calculation points used for drawing exclusion zone isosurface regions, and improving the calculation speed for the selected field points. The aim of this study was to improve performance in both categories.

Methods

For the efficient selection of field points, a higher density of field points is required in areas where the isosurface changes more rapidly. The efficient identification of these areas is done iteratively because the local point density and the shapes of the isosurfaces influence each other. The isosurface is therefore continuously extracted, while increasing the density of field points where necessary.

There are two main reasons for choosing the marching tetrahedron [6] method for non-regular grid isosurface extraction. The first reason is that the marching tetrahedron method allows for fast and efficient adaptive isosurface extraction on a non-regular grid. The second is that a limit can be placed on the degradation of the aspect ratio for the 3-D tetrahedron volume element. This is done by creating the tetrahedral mesh on a body centred cubic lattice. Each level of refinement falls onto a higher density body centred cubic lattice, with interconnecting tetrahedra between the different levels of refinement.

The process for extracting the exclusion zone isosurfaces is started by creating an initial unrefined tetrahedral mesh for each antenna. A mesh is grown from an initial tetrahedron at each antenna origin by adding more tetrahedra to its sides. The process is repeated if the field values on the tetrahedron edges are close to or greater than the isosurface threshold. Mesh structures are merged where antennas are close to each other.

Adaptive mesh refinement is performed after extracting the initial tetrahedral mesh. The refinement criterion is based on how well the extracted isosurface visually represents the actual isosurface. The refinement criterion is met if both the field points on the edges of a short line perpendicularly crossing the centre of an isoface are either above or below the isosurface threshold. This adaptive mesh refinement process continues iteratively until the refinement criterion is met for all isofaces. The process is extremely efficient, as only the tetrahedra close to antennas, or those cut by the isosurface are considered to be refined. A small section of the refined tetrahedral mesh is shown in Figure 1, between a Yagi-Uda and dish antenna. A higher density mesh can be seen in the region where the isosurface changes more rapidly.

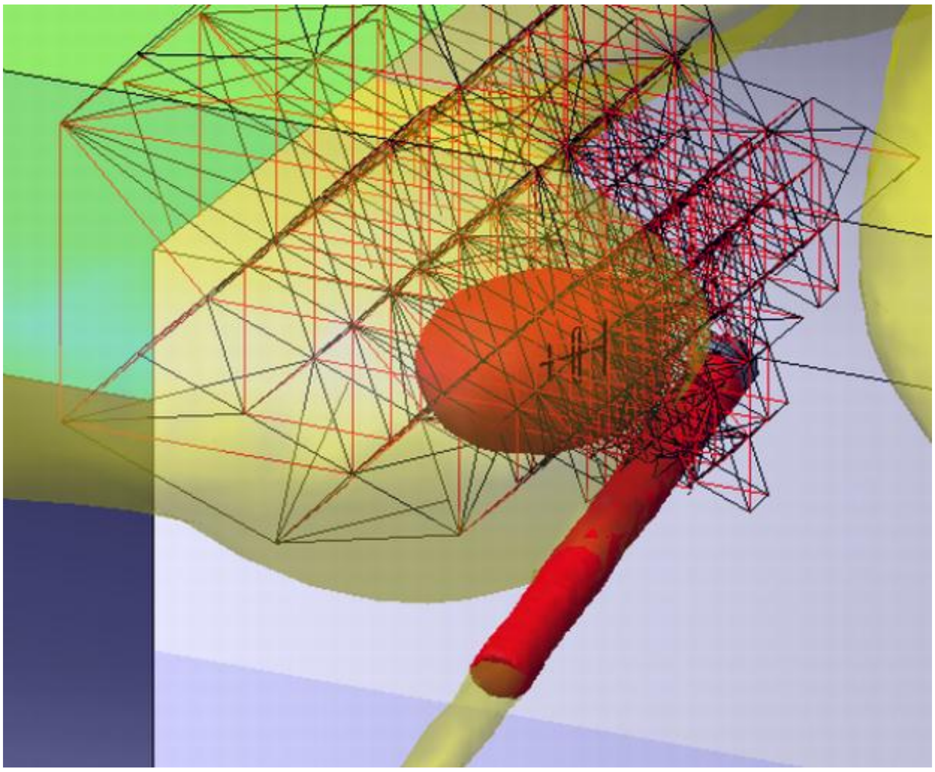

Figure 1: A small section of the refined tetrahedral mesh in the region between a Yagi-Uda and dish antenna

With the efficient selection of field points, the next step in the optimisation process is to increase the calculation speed. The first method for optimising the calculation speed allows the use of a single ray-tracing point source for linear array calculations in the approximate far-field. Normally calculations for linear array antenna models are performed by summation of the complex E-field for each array element, considering the path length, radiation pattern and phase. However, when the calculation point is in the approximate far-field of the antenna, the complex calculation can be done using a single far-field point source.

The spherical gain pattern for a single far-field point source is calculated at the approximate far-field radius for each frequency band. This allows a smooth transition between the two methods. The single point source method allows much faster computation when antennas are placed away from each other. Typical panel or omnidirectional mobile base station antennas have 10 array elements, which can be replaced by a single element when calculating outside a roughly 40m radius at 900 MHz, and 20m radius at 1800 and 2100 MHz.

The far-field point source method is also applied for other kinds of antennas such as Yagi-Uda or folded dipole antennas. These custom antennas are implemented using pre-calculated blocks of E-field values on regular grids, with trilinear interpolation for points in-between. Pre-calculation is performed using full-wave simulation software. Normally the E-field contributed by a custom antenna would be unknown outside its pre-calculated block. With the combination of a far-field point source and a near-field block, the near-field block size can be reduced and valid calculations can be performed anywhere. For antennas with near-field blocks that do not extend up to the approximate far-field boundary, linear interpolation is used to estimate the fields. This provides a smooth transition between the near-field and far-field regions, and provides a conservative estimate in most cases for the expected 1/R decay close to the far-field boundary.

The second method for optimising the calculation speed is the parallelisation of simulation algorithms, so that multithreaded computation can be done. Four parts of the simulation process were identified to be both significant in calculation time and easily parallelisable. The first is the parallel calculation of the spherical far-field gain patterns, for the single point source approximation method. The second is the parallel creation of the initial tetrahedral mesh structures. Mesh structures can be grown in parallel for each antenna, and can be merged when overlapping occurs for antennas that are close to each other. The third is the parallel refinement of the initial meshes, for which public and occupational exclusion zones, as well as non-overlapping exclusion zones can be refined in parallel. The fourth is the breaking down and parallel calculation of long lists of calculation points. This is currently used only for orthoslice calculation, as the adaptive mesh refinement algorithms require only a small number of calculation points to perform each adaptive refinement operation. With the parallelisation of the four parts described here, significant speed improvements were shown with a multithread implementation. There are some memory implications to parallel mesh refinement, as the tetrahedral mesh structures can get quite large. A solution was implemented to reduce the number of threads when the tool runs out of memory.

Results and Conclusions

The algorithms for EMF safety assessment were optimised for efficient selection of the required field calculation points used for drawing exclusion zone isosurface regions, and improving the calculation speed for the selected field points. The optimisation speed was investigated for two scenarios.

The first scenario is a typical base station with five panel antennas, one Yagi and one dish shown in Figure 2. The tri-band panel antennas transmit in the GSM900, DCS1800 and UMTS bands, and have electrical tilt ranges from 0 to 6 degrees. The Yagi-Uda antenna is placed close to the dish, so that different calculation point densities are required in a relatively small volume. The total exclusion zone calculation time was brought down from 3 hours to only 83 seconds.

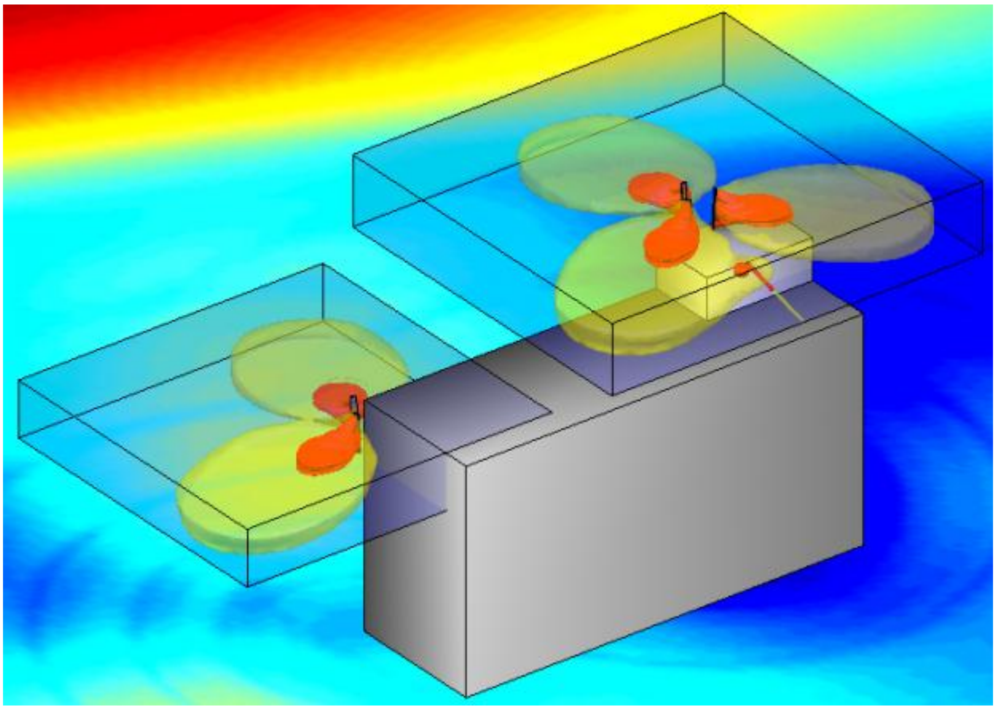

Figure 2: A typical base station illustrating exclusion zone isosurfaces and associated near-field blocks, with a planer E-field orthoslice

The second scenario represents a very large site with fifty tri-band panel antennas without electrical tilt sweep. The exclusion zones for the fifty antennas do not overlap, but the field contribution of each antenna is considered for every calculation point. The total exclusion zone calculation time was brought down from 4.8 hours to only 4.9 minutes.

Table 1 gives a breakdown of the speed improvements for the different optimisation methods for the two sites. The tables also include results for a 200 x 200m orthoslice with 0.1m spacing. The simulations were performed on a personal computer with an Intel® Core™ 2 Quad CPU at 2.4 GHz, with 4 GB RAM, running Windows 7 Enterprise 32 bit.

Base station description	Optimisation method		Total Calculation time		
			Before optimisation	After optimisation	Speedup factor t/t_{opt}
Site with five panel antennas, one dish and one Yagi-Uda antenna	Tetrahedral mesh [1]		3 hours	316 seconds	34
	Linear array far-field point source method		316 seconds	208 seconds	1.5
	Multithreading [2]	exclusion zone extraction	208 seconds	83 seconds	2.5
		orthoslice calculation	33 seconds	16 seconds	2.1
Site with fifty panel antennas	Tetrahedral mesh [1]		4.8 hours	114 minutes	2.5
	Linear array far-field point source method		114 minutes	17.6 minutes	6.5
	Multithreading[2]	exclusion zone extraction	17.6 minutes	4.9 minutes	3.6
		orthoslice calculation	123 seconds	44 seconds	2.8

[1] Compared to uniform grid of points.

[2] Single thread vs. four threads.

Table 1: Simulation speed improvement for optimisation methods

References:

[1] European Union, Directive 2004/40/EC of the European Parliament and of the Council of 29 April 2004 on the minimum health and safety requirements regarding the exposure of workers to the risks arising from physical agents (electromagnetic fields). Official Journal of the European Union, L159, pp1-26, 30 April 2004.

[2] International Commission on Non-ionizing Radiation Protection, Guidelines for limiting exposure to time-varying electric, magnetic, and electromagnetic fields (up 300 GHz). Health Physics, Vol. 74, No. 4, pp. 494-522, 1998.

[3] EMSS Consulting, Technopark, Stellenbosch, 7600, South Africa, http://www.emssixus.com

[4] CENELEC EN 50383, Basic standard for the calculation and measurement of electromagnetic field strength and SAR related to human exposure from radio base stations and fixed terminal stations for wireless telecommunication systems (110 MHz - 40 GHz). June 2010.

[5] IEC 62232 preFDIS, Determination of RF field strength and SAR in the vicinity of radiocommunication base stations for the purpose of evaluating human exposure. Nov 2010.

[6] S. L. Chan and E. O. Purisima. A new tetrahedral tesselation scheme for isosurface generation. Computers and Graphics, 22(1):83–90, 1998.